Bull. Chem. Soc. Ethiop. **2024**, 38(2), 501-509.
DOI: https://dx.doi.org/10.4314/bcse.v38i2.17

ISSN 1011-3924
Printed in Ethiopia
Online ISSN 1726-801X

PREPARATION OF NANOCOMPOSITES FOR CORROSION TREATMENT

Zainab Esmail Sadeq[1], Noor Sabah Al-Obaidi[1], Anfal Salam Al-Mahdawi[1], Ahmed N. Abd[1], Zaid H. Mahmoud[1] and Ban W. Kamal[2]

[1]Department of Chemistry, College of Science, University of Diyala, Iraq
[2]General Directorate of Education of Karkh/1, Ministry of Education, Iraq

(Received October 2, 2023; Revised December 5, 2023; Accepted December 5, 2023)

ABSTRACT. Nano-copper oxide was prepared by utilizing photolysis method and characteristic by using FT-IR, XRD and SEM; the nano size was about 51 nm, environmental impact (pollution reduction) can be improved by using nanostructure particles in preventing corrosion, and nanocomposites have also proven to be an effective alternative to other hazardous and toxic compounds. The results of the current article indicated that the inhibition efficiency increases with increasing concentration of nano-oxide which is added to methyl orange, curcumin, the corrosion rate (CR), inhibition effectiveness were studied at different temperatures. The results showed an increase corrosion rate and a decrease in inhibition efficiency with increase temperature.

KEY WORDS: Corrosion, Inhibitors, Copper oxide, Nanocomposites

INTRODUCTION

Corrosion is described as damage (partial or entire) to an alloy or metal's appearance and performance as a result of the alloy or metal's contact with the medium, whether it is a liquid or a gas [1]. Corrosion is a problem for assets such as (industries, buildings, traffic and railway bridges, and residences) [2, 3]. Corrosion is a natural and spontaneous process that results in the transformation of pure metals and their alloys into a variety of stable forms (sulfides, oxides, nanoxides, hydroxides, etc.) through chemical and electrochemical reactions with their surroundings [4]. As we all know, material corrosion produces a slew of issues in our lives, as well as significant economic, health, and safety consequences. Metals can be protected from corrosion in a variety of ways [5]. For example, various coatings can be used to manage and protect metals from corrosion [6]. Because of their exceedingly tiny grain size and high grain boundary volume percentage, nanostructured materials (1-100 nm) are known for their remarkable mechanical and physical properties [7]. Various facets of nano-scale material synthesis have made significant progress, the emphasis is increasingly turning away from synthesis and toward the creation of functional structures and coatings that are more resistant to the corrosion, iron is widely employed as a construction material in most major industries, including petroleum, food, power generation, chemical industries, and electrochemical industries, owing to its good mechanical qualities and reduce cost, iron main issue is dissolving in acidic and alkaline environments. iron corrosion in concentrated acidic aqueous solutions is a major concern in the most of industries where acids are commonly employed for many applications such as acid cleaning, acid descaling, acid pickling, and oil well acidizing, because of the acid solution's general abrasiveness, construction materials corrode quickly, to prevent metal breakdown and reduce acid usage, corrosion inhibitors must be added [8]. The use of nanotechnology to change the iron/electrolyte contact has been used to lessen the impact of corrosive conditions (e.g production of nanocomposite coatings on Stainless steel) [9-11]. The use of nanomaterials for corrosion control has made significant progress recently, as summarized in [12]. The integration

*Corresponding author. E-mail: noorsabah@uodiyala.edu.iq

of nanoparticles in coatings for better qualities such as corrosion resistance is discussed in this study.

EXPERIMENTAL

Chemicals

All of the reagents, starting substances, chemical solvents were obtained commercially: hydrochloric acid, HCl (1 M); acetone C_3H_6O; benzene, C_6H_6; ammonium hydroxide, NH_4OH (25%); copper nitrate $Cu(NO_3)_2$; ethylene glycol, $C_2H_6O_2$; methyl orange, $C_{14}H_{14}N_3NaO_3S$; and curcumin dye were used as received.

Techniques used for analysis

To analyze the metal surface before and after corrosion in the presence and absence of inhibitors, the scanning electron microscopy (SEM) technique was used. specification of the scanning electron microscope (Model Vega III) made in the Czech, Fourier transform infrared spectroscopy (FTIR) the spectra of compounds were captured using a (Perkin Elmer Speactum- 65 at 400–4000 cm^{-1}) using the KBr disk technique.

Preparation of CuO [13]

The nanoparticles of copper oxide (CuO) were prepared utilizing photolysis method. At the first, (2 g) of copper(II) nitrate ($Cu(NO_3)_2$) was dissolved in (100 mL) distilled water. Then, it was irradiated for (2 h) using the system of UV-irradiation with power (125 W), then the fresh precipitate was separated and washed with acetone for 5 times, and burned at 600 °C.

Preparation of nanocomposite solution

The composites that used in the (coating process) with 100 ppm concentration were prepared by using a natural dye curcumin with copper oxide nanoparticles (nanocomposite) at different concentrations indicates with symbol (Z_1-Z_5) and an organic dye methyl orange with copper oxide nanoparticles (nanocomposite) at different concentrations indicates with symbol (A_1-A_5) as shown in Tables 1 and 2.

Table 1. The proportions of mixing curcumin dye with copper oxide nanoparticles.

No.	Symbol	Curcumin	Copper oxide
1	Z_1	95%	5%
2	Z_2	90%	10%
3	Z_3	85%	15%
4	Z_4	80%	20%
5	Z_5	75%	25%

Table 2. The proportions of mixing methyl orange dye with copper oxide nanoparticles.

No.	Symbol	Methyl orange	Copper oxide
1	A_1	95%	5%
2	A_2	90%	10%
3	A_3	85%	15%
4	A_4	80%	20%
5	A_5	75%	25%

Weight loss procedure

The most common approach for determining corrosion rate and inhibitor performance is the weight loss technique because this method is considered one of the best methods used in most research articles, as it is characterized by accuracy and availability. iron specimens were cleaned using 220, 320, 400, and 600 grit emery paper, then rinsed with running tap water, distilled water, and dried with clean tissue. The specimen was weighed using a four-decimal digital scale, and its dimensions were measured using a vernier to the second decimal of millimeter for 3 hours, a specimen with known surface area and mass is immersed in the test corrosive solution. The mass loss after removing the corrosion products or other deposits from the metal is used to calculate the loss of a metal due to corrosion. The exposed surface area of the specimen and the test period are normally documented along with the mass loss values. The mass loss per unit time per unit area is calculated.

RESULTS AND DISCUSSION

Spectroscopy study

The peak found at 495.9 cm^{-1} in the infrared spectra of copper oxide nanoparticles is a band related with the stretching vibration of Cu-O bonds. The vibration bands within 1602.3 cm^{-1} are CO_2 vibration bands. O-H bonds are represented by vibration bands between 2800 and 3500 cm^{-1} (3428 cm^{-1}). The existence of moisture content is responsible for O-H bonds with very low bands which is due to humidity during the examination. Figure 1 shows that copper oxide was synthesized, which is supported by the presence of a Cu-O bond [14].

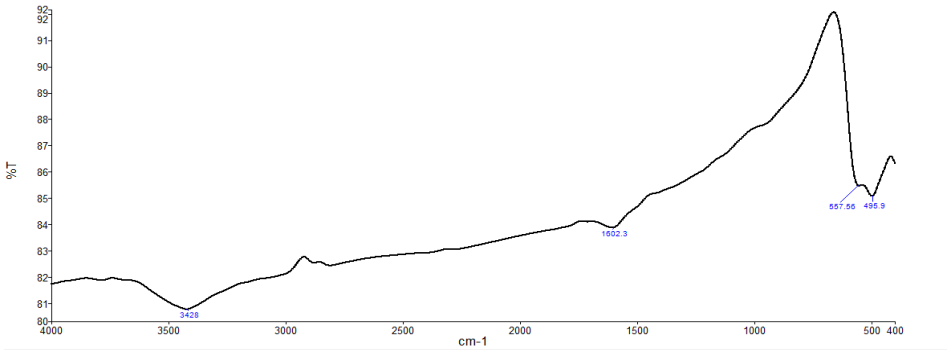

Figure 1. FTIR spectrum of synthesized CuO nanoparticles.

XRD analysis

XRD is used to study phases and crystals structure. The XRD technique was used to determine and confirm the crystal structure of the nanoparticles. X-ray diffraction pattern for (Copper oxide) was shown in Figure 2. The Deby-Sherrer formula listed below was used to calculate the particle sizes [15-18]:

$$D = 0.9\,\lambda/\beta\,\cos\theta \quad (1)$$

Where D: is the crystallite size, λ: is the wave length of radiation, β: is the full width at half maximum (FWHM) and θ: is the Bragg's angle. The estimated particle size of the (copper oxide) is 51.52 nm.

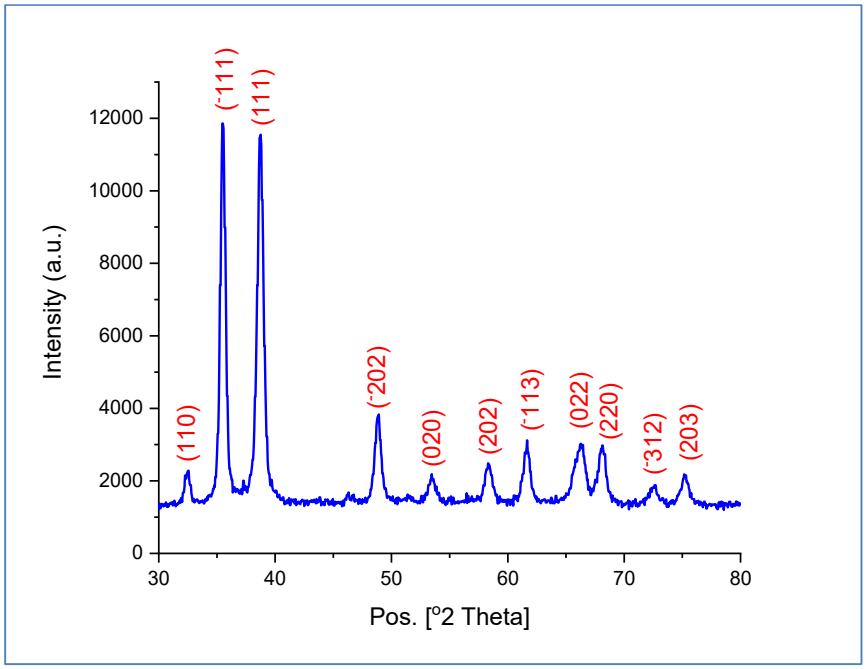

Figure 2. XRD of (CuO) copper oxide nanoparticles.

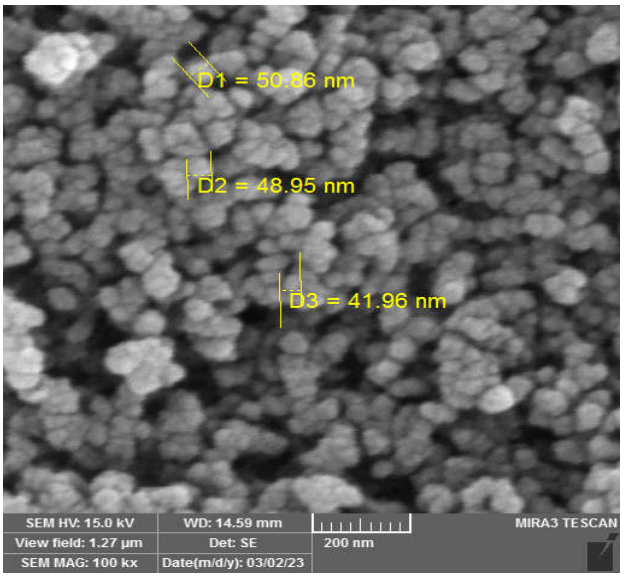

Figure 3. SEM of (CuO) copper oxide nanoparticles.

FE-SEM analysis

The surface morphology of copper oxide nanoparticles was examined by using a scanning electron microscope, and the results showed a large agglomeration of the nanoparticles with smooth surface as shown in Figure 3.

Weight loss measurements

The formula listed below was used for evaluating corrosion rates (CR) both in the absence and presence of inhibiting agents [19]:

$$CR = \frac{\Delta W}{A\,t} \tag{1}$$

ΔW is the amount of weight loss in grams, t is the exposure time in days, and A is the item's area in meters squared. G/m^2 per day (gmd) is a unit of measurement for corrosion rates.
Using the following equation to evaluate inhibition effectiveness:

$$\%\,IE = \frac{CR\ uninh - CR\ inh}{CR\ uninh} \times 100 \tag{2}$$

where CR_{inh} and CR_{uninh} are, respectively, the corrosion rates in the presence and absence of different inhibitor concentrations, at various operating circumstances, inhibitor effectiveness and corrosion rate were assessed; the findings were compiled in Table 3. It is evident that the rate of corrosion (CR) expanded with temperature and reduced with the concentration of an inhibitor [20].

Table 3. Corrosion rate and inhibitor efficiency with different concentration of (nanocomposite) at room temperature.

No.	Name of sample	CR (gmd)	E%
1	Blank	225.149	
2	Z_1	43.75	80.56
3	Z_2	33.185	85.26
4	Z_3	32.11	85.73
5	Z_4	26.007	88.44
6	Z_5	20.592	90.85
7	A_1	29.16	87
8	A_2	19.093	91.51
9	A_3	18.427	91.81
10	A_4	15.364	93.17
11	A_5	3.452	98.46

We note that the presence of CuO with (curcumin and methyl orange) caused a reduction in corrosion and an improvement in coatings' effectiveness. Numerous studies have demonstrated that coatings are just one of the common ways to shield metals against the effects of acidic conditions and salty [21-23].

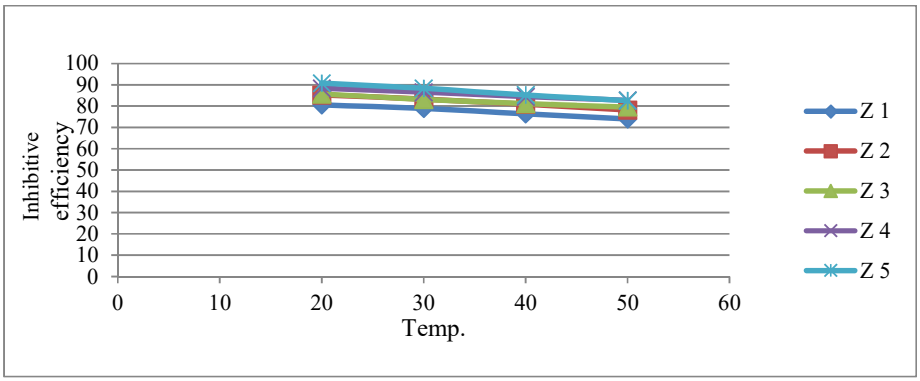

Figure 4. The effect of increase temperature on inhibitive efficiency of (CuO – curcumin).

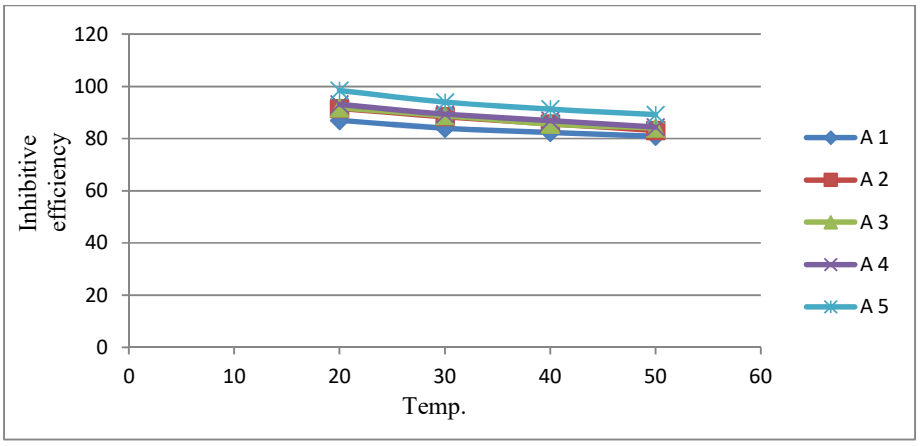

Figure 5. The effect of increase temperature on inhibitive efficiency of (CuO – methyl orange).

Figure 4 and 5 show the effect change in temperature on the corrosion rate (CR) with different amount concentrations of nanocomposites, and these data show that increases temperature that raise rate of chemical reactions [24] high temperatures have many effects on chemical reactions, which have increased rates with an increase in temperature from (293, 303, 313, and 323 K) [25-29].

Inhibitor performance and adsorption studies

It has been demonstrated that raising concentrations of inhibitors ranging from 20 to 100 ppm reduces the corrosion rate to extremely low levels. The adsorption mechanism can be studied using the corrosion rate data.

Langmuir adsorption isotherm

Using the equation 3 to calculate (Langmuir adsorption isotherm),

$$\frac{Ci}{\theta} = \frac{1}{KI} + \text{ci} \qquad (3)$$

Figure 6 shows plots of ($\frac{Ci}{\theta}$) versus (Ci) for (CuO – methyl orange) and (CuO-curcumin) at different temperature. The data given was linear, demonstrating the Langmuir isotherm shows that inhibitors are absorbed, It might also provide an explanation for the increase in inhibitor effectiveness brought on by an increase in the number of inhibitor molecules that adsorb on surfaces [30]. K_L values that can be calculated from the straight-line intercept can be, and then substituted in equation to calculate ΔG^o ads and correlation coefficient (R^2). The inhibitor adsorption equilibrium constant K_L values rise as the temperature rises. The stronger adsorption was amply demonstrated by the higher K_L values. From observing the R_2 values, we find that the highest value (0.999) is close to the correct one, evidence of absorption following Lanckmuir's law.

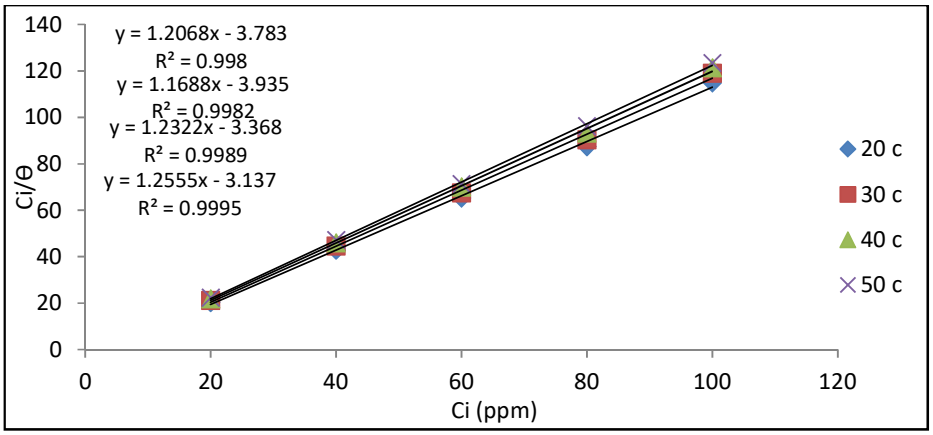

Figure 6. Langmuir adsorption isotherm of (CuO – methyl orange).

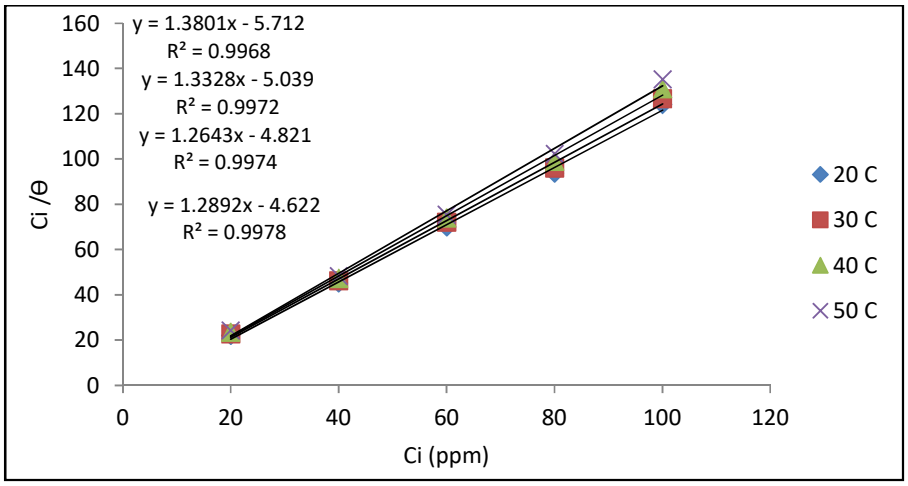

Figure 7. Langmuir adsorption isotherm of (CuO – curcumin).

CONCLUSION

In this study, copper oxide nanoparticles were prepared using photolysis method. The method of coating the metal by prepared nanocomposites (nano-oxide + dye) was also chosen, and the results indicated that a protection for the metal surface occurred after coating it with the above-prepared nano-composites. It was found that the increase in the inhibition efficiency is directly proportional to the increase in the percentage of nano-oxide in the prepared compounds.

ACKNOWLEDGEMENTS

The authors would like to thank Department of Chemistry, College of Science, University of Diyala for continuous support and facilities.

REFERENCES

1. Deab, H.B.; Abd, A.N.; Hassan, K.H. Corrosion prevention of industrially used metal using green inhibitor and nano composites. *J. Crit. Rev.* **2020**, 7, 3879-3888.
2. Yang, H.Q.; Zhang, Q.; Tu, S.S.; Wang, Y.; Li, Y.M.; Huang, Y. Effects of inhomogeneous elastic stress on corrosion behaviour of Q235 steel in 3.5% NaCl solution using a novel multi-channel electrode technique. *Corros. Sci.* **2016**, 110, 1-14.
3. Dhaundiyal, P.; Bashir, S.; Sharma, V.; Kumar, A. An investigation on mitigation of corrosion of mildsteel by Origanum vulgare in acidic medium. *Bull. Chem. Soc. Ethiop.* **2019**, 33, 159-168.
4. Mai, W.; Soghrati, S.; Buchheit, R.G. A phase field model for simulating the pitting corrosion. *Corros. Sci*. **2016**, 110, 157-166.
5. Khalil, M.W.; Eldin, T.A.S.; Hassan, H.B.; El-Sayed, K.; Hamid, Z.A. Electrodeposition of Ni–GNS–TiO_2 nanocomposite coatings as anticorrosion film for mild steel in neutral environment. *Surf. Coat. Technol*. **2015**, 275, 98-111.
6. Cui, X.; Zhu, G.; Pan, Y.; Shao, Q.; Dong, M.; Zhang, Y.; Guo, Z. Polydimethylsiloxane-titania nanocomposite coating: Fabrication and corrosion resistance. *Polymer* **2018**, 138, 203-210.
7. Ramachandra, M.; Maruthi, G.D.; Rashmi, R. Evaluation of corrosion property of aluminium-zirconium dioxide ($AlZrO_2$) nanocomposites. *Int. J. Mater. Metallurg. Eng.* **2016**, 10, 1321-1326.
8. Hameed, R.A.; Abu-Nawwas, A.A.H.; Shehata, H.A. Nano-composite as corrosion inhibitors for steel alloys in different corrosive media. *Adv. Appl. Sci. Res.* **2013**, 4, 126-129.
9. Murali, V.N.; Starvin, M.S.; Raj, J.B. Exploring the corrosion inhibition of magnesium by coatings formulated with nano CeO and ZrO particles. *Bull. Chem. Soc. Ethiop*. **2023**, 37, 1299-1306.
10. Dominic, O.O.; Chikaodili, A.V.; Sandra, O.C. Optimum prediction for inhibition efficiency of *Sapium ellipticum* leaf extract as corrosion inhibitor of aluminum alloy (AA3003) in hydrochloric acid solution using electrochemical impedance spectroscopy and response surface methodology. *Bull. Chem. Soc. Ethiop*. **2020**, 34, 175-191.
11. Zoromba, M.S.; Belal, A.A.M.; Al-Hussaini, A.S. From copolymer precursor to metal oxides nanoparticles: Synthesis and characterization of doped copper and cobalt copolymer via in situ and ex situ copolymerization. *J. Macromol. Sci. Part A* **2015**, 52, 394-400.
12. Abeng, F.E.; Ikpi, M.E.; Anadebe, V.C.; Emori, W. Metolazone compound as corrosion inhibitor for API 5L X-52 steel in hydrochloric acid solution. *Bull. Chem. Soc. Ethiop*. **2020**, 34, 407-418.
13. Al-Obaidi, N.S.; Mahmoud, Z.H.; Ali, A.A.F.A.S.; Ali, F.K. Evaluating the electric properties of poly aniline with doping ZnO and α-Fe_2O_3 nanoparticles. *Pharmacophore* **2018**, 9, 61-67.

14. Sawant, S.S.; Pawar, V.; Janrao, S.; Yamgar, R.S.; Nivid, Y. Synthesis and characterization of transition metal complexes of novel Schiff base 8-[(z)-[3-(n-methylamino) propyl] iminomethyl]-7-hydroxy-4-methyl-2h-chromen-2-one][nmapimhmc] and their biological activities. *Int. J. Res. Pharm. Chem*. **2013**, 3, 636-644.
15. Zhang, T.Y.; Zhang, D. Aqueous colloids of graphene oxide nanosheets by exfoliation of graphite oxide without ultrasonication. *Bull. Mater. Sci*. **2011**, 34, 25-28.
16. Mahmood, J.M.; Mahmoud, Z.H.; Al-Obaidi, N.S.; Rahima, A.M. Gama-Fe_2O_3 silica-coated 2-(2-benzothiazolyl azo)-4-methoxyaniline for supercapacitive performance. *J. Electrochem. Sci. Eng.* **2023**, 13, 521-536.
17. Mahmoud, Z.H.; Ahmed, N.S.; Shamkhi, W.; Dha'a, O. Nanoparticles: A review of preparation and characterization of nanoparticles with application. *Earthline J. Chem. Sci*. **2020**, 3, 141-149.
18. Al-Obaidi, N.S.; Mustafa, S.N. Synthesis, characterization and electrical study of poly aniline doping with nano silver oxide. *Int. J. Pharm. Res.* **2020**, 12, 1038-1044.
19. Yaro, A.S.; Abdul-Masih, N.S.; Kadhim, A.A. The influence of temperature on corrosion inhibition of carbon steel in air-saturated 7N H_3PO_4 by potassium iodide. *Iraqi J. Chem. Petrol. Eng.* **2000**, 1, 83-87.
20. Nnabuka, E.O.; Awe, F. Experimental and quantum chemical studies on ethanol extract of *Phyllanthus amarus* (EEPA) as a green corrosion inhibitor for aluminum in 1 M HCl. *Portugal. Electrochim. Acta* **2018**, 36, 231-247.
21. Ćurković, L.; Ćurković, H.O.; Salopek, S.; Renjo, M.M.; Šegota, S. Enhancement of corrosion protection of AISI 304 stainless steel by nanostructured sol–gel TiO_2 films. *Corros. Sci*. **2013**, 77, 176-184.
22. Silva, P.S.D.; Costa, A.N.; Mattos, O.R.; Correia, A.N.; Lima-Neto, P.D. Evaluation of the corrosion behavior of galvannealed steel in chloride aqueous solution and in tropical marine environment. *J. Appl. Electrochem*. **2006**, 36, 375-383.
23. Chaubey, N.; Singh, V.K.; Quraishi, M.A.; Ebenso, E.E. Corrosion inhibition of aluminium alloy in alkaline media by *Neolamarkia cadamba* bark extract as a green inhibitor. *Int. J. Electrochem. Sci.* **2015**, 10, 504-518.
24. Khadom, A.A.; Yaro, A.S.; Kadum, A.A.; AlTaie, A.S.; Musa, A.Y. The effect of temperature and acid concentration on corrosion of low carbon steel in hydrochloric acid media. *Am. J. Appl. Sci.* **2009**, 6, 1403.
25. Abakedi, O.U. Aluminum corrosion inhibition by *Microdesmis puberula* leaf extract in 2 M hydrochloric acid solution. *Int. J. Innov. Res. Sci. Eng. Technol*. **2017**, 5, 6-14.
26. Beda, R.H.B.; Niamien, P.M.; Bilé, E.A.; Trokourey, A. Inhibition of aluminium corrosion in 1.0 M HCl by caffeine: Experimental and DFT studies. *Adv. Chem.* **2017**, 6975248.
27. Raghavendra, N.; Bhat, J.I. Anti-corrosion properties of areca palm leaf extract on aluminium in 0.5 M HCl environment. *South Afr. J. Chem.* **2018**, 71, 30-38.
28. Fouda, A.S.; Elewady, G.Y.; Shalabi, K.; Habouba, S. Anise extract as green corrosion inhibitor for carbon steel in hydrochloric acid solutions. *Int. J. Innov. Res. Sci. Eng. Technol*. **2014**, 3, 2319-8753.
29. Fouda, A.S.; Abdallah, M.; Ahmed, I.S.; Eissa, M. Corrosion inhibition of aluminum in 1 M H_3PO_4 solutions by ethanolamines. *Arab. J. Chem.* **2012**, 5, 297-307.
30. Diki, N.Y.S.; Bohoussou, K.V.; Kone, M.G.R.; Ouedraogo, A.; Trokourey, A. Cefadroxil drug as corrosion inhibitor for aluminum in 1 M HCl medium: Experimental and theoretical studies. *IOSR J. Appl. Chem*. **2018**, 11, 24-36.